

MODE EXCITATION IN A GYROTRON  
OPERATING AT THE FUNDAMENTAL

K. E. Kreischer, R. J. Temkin

October 1980

PFC/JA-80-22

MODE EXCITATION IN A GYROTRON  
OPERATING AT THE FUNDAMENTAL \*

K. E. Kreischer, R. J. Temkin

Plasma Fusion Center †  
Massachusetts Institute of Technology  
Cambridge, Massachusetts 02139

A simplified formalism has been developed for calculating the minimum starting currents of gyrotron modes, as well as the sequence of gyrotron modes excited as a function of resonator magnetic field. Unlike treatments which assume that modes are excited at the Doppler-shifted cyclotron frequency, this analysis is in good agreement with the exact solution of gyrotron linear theory. It is shown that each  $TE_{mpq}$  mode is characterized by  $q$  strong excitation branches, and of these branches two predominate for  $q \geq 2$ . For the case of  $q = 1$ , only a single branch at the Doppler down-shifted frequency is strong. The cyclotron frequencies at which these branches are excited are found to vary with  $q$ , but their minimum starting currents are roughly independent of  $q$  if  $Q$  does not depend on  $q$ . A simple technique for constructing mode spectra is presented, and examples are given for the  $TE_{031}$  and  $TE_{521}$  modes. In addition the effect of the time-varying gun voltages on the mode excitation spectra during the turn-on phase of a pulsed gyrotron has been investigated. The method in which the cathode and control anode voltages of the gun are increased to their final operating values can significantly affect which modes are excited in a gyrotron. Of the two startup procedures analyzed in detail, it was found that holding the cathode voltage steady at its final value while ramping-up the anode voltage helped to minimize the appearance of parasitic

\* Work supported by U.S.D.O.E. Contract DE-AC-02-80ER52059

† Supported by U.S. Department of Energy

modes. This observation is based on the fact that the resonance condition is less sensitive to changes of the anode voltage than to cathode voltage variations.

Key words: gyrotron theory, microwave tube theory, electron cyclotron maser, millimeter wave source.

## 1. Introduction

The gyrotron or electron cyclotron maser has proven to be an efficient source of high power millimeter wave radiation (1,2). For high power, high frequency gyrotrons, operation in relatively large resonators may be required to limit cavity heating and reduce cavity losses. In such resonators, the operating mode will be of higher order, and mode separation will be small. This may lead to excitation of parasitic modes or to multimode operation, limiting gyrotron operation and efficiency.

In this paper, we analyze the spectrum of modes excited in a gyrotron resonator. A formalism is developed which describes the basic features of mode excitation, including the magnetic field value at which a given mode may be excited with a minimum beam current. This formalism is based on a previously derived linear theory of gyrotron threshold operation (3). The application of this theory to mode excitation is presented in Section 2. First, the basic principles of mode excitation in a gyrotron resonator are reviewed. It is shown that mode excitation in a gyrotron resonator is qualitatively different from that in a gyrotron travelling wave amplifier. It is also shown that the simple, often used approximation that modes are excited at a Doppler shifted cyclotron resonance is not sufficiently accurate for developing a realistic picture of mode excitation. In our analysis, a more rigorous formalism based on the exact linear theory (3) first relates the magnetic field and beam current needed for self-oscillation of each  $q \neq 1$   $TE_{mpq}$  mode to the field and current of the nearby  $TE_{mp1}$  mode. Then, the various modes with different transverse mode numbers  $m$  and  $p$  are related to one another. This gives a reasonably accurate description of the sequence of modes excited in a resonator as the magnetic field is varied, as well as the starting currents required to excite them. Section 2 ends with a comparison of our semi-quantitative theory with both the simple Doppler approximation and exact numerical solutions. Examples are also given of typical mode spectra for a gyrotron operating at 140 GHz.

In Section 3, the time-dependent behavior of the gyrotron during the turn-on phase is investigated. Two different methods of pulsed gyrotron turn-on are considered in detail. In one method, the voltages on the cathode (U) and first anode ( $V_a$ ) are driven negative such that ( $V_a/U$ ) is held constant. In the second method, U is held constant at its final value and  $V_a$  is varied from zero to its final operating value. These two methods of voltage variation are found to produce significantly different mode excitation results. Such differences may be important in gyrotrons operating in higher modes where mode spacing is small.

Finally, a summary of the conclusions of our paper is presented in Section 4.

## 2. Theory of Mode Excitation

In this section, we will derive the magnetic field and minimum starting current required for self-oscillation of a gyrotron operating at the fundamental in a TE mode. The simple approximations often used to predict mode excitation will be outlined in subsection 2A. A more accurate theory will be derived in subsection 2B. Finally, this new theory will be compared with exact numerical solutions and examples of mode spectra will be presented in subsection 2C.

### 2A. Basic Theory

In the electron cyclotron maser, the interaction between an RF wave ( $\omega, \bar{k}$ ) and an electron beam ( $\bar{v}$ ) is optimized near the Doppler shifted cyclotron resonance condition (1),

$$\omega - \bar{k} \cdot \bar{v} = \omega_c \quad (1)$$

$$\omega_c = eB/\gamma m_e c \quad (2)$$

$$\gamma = (1 - v^2/c^2)^{-1/2} \quad (3)$$

Defining the electron beam velocity along the magnetic field axis (z-axis) as u and the projection of the RF wave momentum on that axis as  $k_{||}$ , Eq. (1) becomes

$$\omega \pm k_{\parallel} u = \omega_c \quad (4)$$

where the  $-(+)$  sign refers to forward (backward) propagation of the electron beam with respect to the direction of the RF travelling wave. In a travelling wave gyrotron amplifier, only one sign in Eq. (4) would generally apply, depending on whether the amplifier was a forward  $(-)$  or backward  $(+)$  wave amplifier. In a gyrotron oscillator, the RF field is a standing wave in the axial direction. Since a standing wave can be decomposed into waves travelling in both the forward and backward directions, a gyrotron oscillator can, in principle, be excited at both the  $(+)$  and  $(-)$  resonances of Eq. (4). In fact, as will be described in detail below, this is roughly correct for a  $TE_{mpq}$  gyrotron oscillator mode as long as the axial mode number,  $q$ , is equal to or greater than 2. For  $q = 1$ , usually the case of most interest, the gyrotron oscillator is only excited at the forward wave resonance, given by the  $(-)$  sign in Eq. (4).

In general, it is convenient to define a dimensionless parameter  $x$  which is proportional to the magnetic field:

$$x \equiv \frac{\omega_c - \omega}{k_{\parallel} u} \quad (5)$$

The resonance condition, Eq. (4), can then be rewritten as  $x = \pm 1$ . For a  $TE_{mp1}$  mode, the forward wave resonance occurs at  $x = -1$ . A gyrotron operating in a  $TE_{mp1}$  mode typically has a gain bandwidth extending from approximately  $x = 0$  to  $-3.0$  (3). Although Eq. (4) indicates that the highest gain for this device should be achieved at  $x = -1$ , nonlinear theory shows that the optimum efficiency occurs at a somewhat smaller value of  $x$ , usually in the range  $-3.0 \leq x \leq -1.5$ .

A second condition required to analyze mode excitation is the cavity resonance equation. We will assume the resonator is a right circular cylinder of radius  $R_0$  and length  $L$  with a sinusoidal longitudinal profile of the RF field. The parallel and perpendicular wavenumbers,  $k_{\parallel}$  and  $k_{\perp}$ , of the RF field of such a cavity will be independent of the axial coordinate. Although a more realistic cavity might include allowance for output coupling and tapering of the cavity walls, the results of this paper based on this simple cavity should be qualitatively valid for a gyrotron with a more complex cavity design. The resonance condition for a  $TE_{mpq}$  mode in a circular cylindrical cavity can be written as:

$$\left(\frac{\omega}{c}\right)^2 = k^2 = k_{\perp}^2 + k_{\parallel}^2 \quad (6)$$

where

$$k_{\perp} = \frac{v_{mp}}{R_o} \quad (7)$$

$$k_{\parallel} = \frac{q\pi}{L}$$

and  $v_{mp}$  is the  $p^{\text{th}}$  root of  $J_m^1(x) = 0$ . In a gyrotron, the cavity is ordinarily designed to reduce the importance of the Doppler effect by maintaining  $k_{\parallel} \ll k_{\perp}$  (1). In such a case, we may approximate Eq. (6) by:

$$\frac{\omega}{c} = k = \frac{v_{mp}}{R_o} \left[ 1 + \frac{1}{2} \frac{q^2 \pi^2 R_o^2}{v_{mp}^2 L^2} \right] \quad (8)$$

Once the cavity and electron beam parameters ( $R_o$ ,  $L$ ,  $u$  and  $v$ ) and the mode of operation ( $TE_{mpq}$ ) are set, it is possible to determine the approximate value of magnetic field needed for device operation. Eq. (6) is first solved to obtain the oscillation frequency  $\omega$ , and this value is used in Eq. (4) to calculate  $\omega_c$  and subsequently the magnetic field. Although this simple analysis allows one to quickly determine the major excitation regions of a gyrotron, it is not accurate enough for a quantitative analysis, as will be shown in the next section.

## 2B. Mode Excitation Analysis

We wish to calculate the threshold operating current and the emission frequency of a gyrotron oscillator as a function of magnetic field and applied voltage. The exact solution of this problem requires an analysis of both a power balance equation to determine the starting current and a frequency detuning equation to determine the oscillation frequency of the resonator (3). If we assume a high  $Q$  cavity, then we may ignore the frequency detuning equation. This simplification introduces a fractional error of approximately  $Q^{-1}$  to the oscillation frequency. As a result of this assumption the frequency can be calculated using Eqs. (6) and (7), or alternatively Eq. (8). For determining the mode excitation vs. magnetic field, we must use the starting current equation instead of the simple cyclotron resonance condition, Eq. (4).

Assuming no spread in velocity and a right circular cylinder cavity, we have for a TE<sub>mpq</sub> mode (3):

$$I_{st} = -2\epsilon_0 \frac{\omega}{Q_T} |p_0|^2 \frac{m_e}{e} \frac{(k_{||} u)^2}{G(r_e)} \left[ F_c - \frac{1}{2} \frac{sw^2}{c^2} \frac{dF_c}{dx} \right]^{-1}$$

$$|p_0|^2 = \frac{\pi L}{2} k_{\perp}^{-2} \left[ v_{mp}^2 - m^2 \right] J_m^2(v_{mp})$$

$$G(r_e) = J_{m\pm 1}^2(k_{\perp} r_e) \quad (9)$$

$$F_c(x, q) = \frac{2}{(1-x^2)^2} \sin^2 \left( \frac{(x+1)\pi q}{2} \right)$$

$$s = \omega_c / k_{||} u$$

and  $Q_T$  is the overall cavity Q.

The spacing in magnetic field (or  $x$ ) of two different modes (mpq) and ( $m'p'q'$ ) can be analyzed by separately considering differences in transverse (mp) and axial (q) mode numbers. If two modes differ only in axial mode number, that is  $m = m'$ ,  $p = p'$ ,  $q \neq q'$ , then the mode spacing is small since the  $q$  dependence of the mode frequency, Eq. (8), is

$$\frac{q^2 \pi^2 R_0^2}{2v_{mp}^2 L^2} \approx \frac{q^2 \lambda^2}{8 L^2} \ll 1 \quad (10)$$

and the  $q$  dependence of the Doppler shift in Eq. (4) is

$$\frac{k_{||} u}{\omega} \approx \frac{q \lambda}{2 L} \beta_{||} \ll 1 \quad (11)$$

However, modes which have the same axial mode number ( $q = q'$ ) but differ in transverse mode number have a frequency spacing which depends primarily on the difference between  $v_{mp}$  and  $v_{m'p'}$ . Since  $v_{mp}$  and  $v_{m'p'}$  vary widely, this mode spacing may be either small or large. Hence, in the following analysis, it will be convenient to first determine the starting current and the frequency spacing of TE<sub>mpq</sub> and TE<sub>m'p'q'</sub> modes with  $q$  and  $q' > 1$  relative to the modes

$TE_{mp1}$  and  $TE_{m'p'1}$  respectively. The frequency difference of the  $TE_{m'p'1}$  mode relative to  $TE_{mp1}$  can then be calculated using the following relation:

$$\frac{\Delta\omega}{\omega} \approx \frac{v_{m'p'} - v_{mp}}{v_{mp}} \approx \frac{\Delta\omega_c}{\omega_c}$$

This approach permits a simple and straightforward method of determining the sequence of modes excited in a given cavity as the magnetic field is varied.

In order to use this methodology, one must identify the dependence of  $I_{st}$  on the parameters  $q$  and  $x$ , the latter determining the magnetic field through the parameter  $\omega_c$  (see Eq. (5)). In Eq. (9),  $G(r_e)$  is determined only by the transverse RF field structure and thus has no dependence on  $q$ . The parameter  $|p_0|^2$  which depends on the stored energy in the cavity is also independent of  $q$  and magnetic field. The major dependence on  $x$  and  $q$  derives from the parameters  $k_{||}$ ,  $Q_T$ ,  $s$  and  $F_c(x, q)$ . In general, the dependence of  $Q_T$  on  $q$  is a function of the cavity shape. It is particularly sensitive to cavity tapering (4). For simplicity, in the present analysis we will obtain an approximate expression for the  $q$  dependence of  $Q_T$ . We assume that the overall  $Q$ ,  $Q_T$ , is nearly equal to the output coupling or diffractive  $Q$ ,  $Q_D$ . Then, as discussed by Vlasov et al. (4),

$$Q_T \approx Q_D = \frac{4\pi L^2}{q^2 \lambda^2} \frac{1}{1 - |R_1 R_2|} \quad (12)$$

where  $R_1, R_2$  are the voltage reflection coefficients at the cavity ends. One cavity end will generally be totally reflecting,  $|R_1| \approx 1$ , while the other cavity end will have  $|R_2| < 1$  for output coupling. In the present analysis, we will assume that the dependence of  $Q_T$  on  $q$  is given by:

$$Q_T \approx q^{-2} Q_1$$

where  $Q_1$  is the  $Q_D$  of the  $q = 1$  mode ( $TE_{mp1}$ ). Introducing a parameter  $y$ :

$$y \equiv \frac{\omega_c L}{2\pi c} \frac{w^2}{uc} \approx \frac{\omega L}{2\pi c} \frac{w^2}{uc} = \frac{L}{\lambda} \frac{w^2}{uc}$$



we may rewrite Eq. (9) as:

$$I_{st} = \left[ \frac{2\epsilon_0}{Q_1} |p_0|^2 \frac{m_e}{e} \frac{1}{G(r_e)} \left( \frac{\pi}{L} \right)^2 \right] \frac{(u^2 \omega q^4)}{\left( \frac{y}{q} \frac{dF_c}{dx} - F_c \right)} \quad (13)$$

We will now relate the starting current and magnetic field values for the  $TE_{mpq}$  modes with  $q > 1$  to the values for the  $TE_{mp1}$  mode. The minimum starting current values are obtained by minimizing  $I_{st}$  with respect to  $x$ . Near such minima, for beam energies exceeding a few keV, it can be shown that the term  $F_c(q, x)$  is small and may be omitted. Then we may rewrite Eq. (13) as:

$$I_{st} \approx \left[ \frac{4\epsilon_0}{Q_1} |p_0|^2 \frac{m_e}{e} \frac{c^2}{G(r_e)} \left( \frac{\pi}{L} \right)^3 \right] \left( \frac{u^3}{w^2} \right) \frac{q^5}{dF_c/dx} \quad (14)$$

Eq. (14) is the form required for analysis of mode excitation. The minima of Eq. (14), obtained by finding the maxima of  $dF_c(q, x)/dx$ , and the corresponding values of  $I_{st}$  and magnetic field ( $x$ ), are listed in Table 1 in order of increasing  $I_{st}^{MIN}$ .

The results in Table 1 may be compared to the predictions of the basic theory described earlier in this section. Eq. (4) predicts that the modes should be excited at

$$x = \frac{\omega_c - \omega}{k_{||} u} = \pm 1 \quad (\text{basic theory})$$

Table 1 indicates that the basic theory is reasonably accurate at large  $q$ . However, for  $q = 1$ , there is only one strong mode, near the forward wave resonance at  $x = -1.1$ . For  $q = 2$ , the backward wave resonance is stronger than the forward wave and it is located at  $x = 0.4$ , well shifted from the value  $x = 1$  predicted by Eq. (4).

In general, for any  $TE_{mpq}$  mode, as the magnetic field is varied, the mode may be excited at an infinite series of magnetic field values. Most of these excitation regions or branches require very high starting currents. They correspond to higher order excitation processes in which the electron beam, in traversing the cavity, loses and gains energy several times in a cyclic fashion. An example of such

a higher order excitation is the  $TE_{mp1}$  mode excited at  $x = 3.3$ , the last entry in Table 1.

Table I

TE <sub>mpq</sub> Mode Excitation in a Gyrotron Oscillator			
q	x <sub>MIN</sub>	I <sub>ST</sub> <sup>MIN</sup> (q)	Q <sub>T</sub> I <sub>ST</sub> <sup>MIN</sup> (q)
		I <sub>ST</sub> <sup>MIN</sup> (q=1)	Q <sub>1</sub> I <sub>ST</sub> <sup>MIN</sup> (q=1)
1	-1.1	1.0	1.0
2	0.4	3.9	0.98
2	-1.25	4.8	1.2
3	0.67	9.7	1.08
3	-1.2	11.0	1.22
4	0.75	17.7	1.11
4	-1.18	19.5	1.22
5	0.82	28.3	1.13
5	-1.14	30.5	1.22
3	-0.17	32.5	3.61
6	0.83	41.0	1.14
6	-1.12	43.6	1.21
7	0.86	56.6	1.16
7	-1.1	59.5	1.21
1	3.3	60.8	60.8

Disregarding these higher order excitations, each  $TE_{mpq}$  mode is found to have q strong excitation branches located roughly in the region  $-1 \leq x \leq 1$ . Of these q branches, for  $q \geq 2$ , there are two branches that are significantly stronger than the other branches. These branches occur at  $x \approx \pm 1$  for large q, but may be significantly shifted at small q. These two strong branches account for virtually all of the excitation values in Table 1, the only exceptions being the tenth and fifteenth entries.

One important result evident in Table 1 is that the minimum starting current increases as  $q^2$ . However, this  $q^2$  dependence is totally the result of our earlier assumption that the cavity Q,  $Q_T$ , decreases at  $q^{-2}$   $Q_1$ . If we eliminate this assumption, as is done in the last column of Table 1, we find that the starting current of a  $TE_{mpq}$  mode is

essentially independent of  $q$ . That is, if the cavity output coupling is adjusted so as to maintain  $Q_T$  constant for all values of  $q$  the modes  $TE_{mp1}$ ,  $TE_{mp2}$ ,  $TE_{mp3}$ , etc. all have about the same minimum starting current and gain.

## 2C. Gyrotron Mode Spectra

In order to construct a mode chart, the minimum starting current and magnetic field required to excite each mode must be calculated. The magnetic field, expressed in terms of  $\omega_c$ , can be determined using Eq. (5). If we denote  $\omega_c(q, x_{MIN})$  to be the cyclotron frequency associated with the minimum starting current of a  $TE_{mpq}$  mode, then  $\omega_c(q, x_{MIN})$  can be related to the excitation of the  $TE_{mp1}$  mode at  $x = -1.1$ ,  $\omega_c(1, -1.1)$ , by:

$$\frac{\omega_c(q, x_{MIN}) - \omega_c(1, -1.1)}{(\pi u/L)} = qx_{MIN} + 1.1 + \frac{(q^2 - 1) \lambda c}{4 L u} \quad (15)$$

The last term in Eq. (15) is the correction due to the  $q$  dependence of  $\omega$ . It is generally a significant correction, resulting in a shift of all the  $q > 1$  modes to higher magnetic fields.

The minimum starting current is obtained from Eq. (14). As above,  $I_{ST}^{MIN}$  of  $q > 1$  modes will be related to  $I_{ST}^{MIN}$  of the  $q = 1$  mode. The two factors that must be considered are  $q^5/(dF_c/dx)$  and  $u^3/w^2$ . The former can be determined from the tabulated results of Table 1. The latter depends on the characteristics of the magnetron injection type guns presently used in gyrotrons. Assuming adiabatic theory, the quantity  $w^2$  will increase linearly as the magnetic field is increased. By conservation of energy,  $u$  will simultaneously decrease so that  $(u^2 + w^2)$  is constant. This implies that  $(u^3/w^2)$ , and therefore  $I_{ST}$ , will decrease strongly with increasing magnetic field. Denoting parameters associated with the  $TE_{mp1}$  mode with a zero subscript, and defining  $g \equiv w/u$ , then the ratio  $(u^3/w^2)$  for  $q > 1$  modes can be written as:

$$\frac{u^3}{w^2} \approx \left( \frac{u_0^3}{w_0^2} \right) \left[ 1 - \left( 1 + \frac{3}{2} g_0^2 \right) \frac{\Delta\omega_c}{\omega_c} \right] \quad (16)$$

where  $\Delta\omega_c \equiv [\omega_c(q, x_{MIN}) - \omega_c(1, -1.1)]$  is obtained from Eq. (15). Using this result, the starting current of  $q > 1$

modes can be calculated as follows:

$$I_{ST}^{MIN} = \left[ I_{ST}^{MIN} (q = 1) \right] \cdot \left[ 1 - \left( 1 + \frac{3}{2} g_0^2 \right) \frac{\Delta\omega_c}{\omega_c} \right] \cdot \left[ \frac{I_{ST}^{MIN}}{I_{ST}^{MIN} (q = 1)} \right] \quad (17)$$

where the ratio in the last bracket can be found in Table 1. An entire mode spectrum can now be developed by calculating  $I_{ST}$  and  $\omega_c$  for  $q = 1$  modes, and then using Eqs. (15) and (17) to determine the corresponding values for  $q > 1$  modes.

In Figure 1, the semi-quantitative theory just derived is compared with an exact numerical calculation of the starting current vs. magnetic field using Eq. (9). The points denoted by (x) were calculated using Eqs. (15) and (17). The agreement is found to be quite good, especially for the strong branches of the lower  $q$  modes. As can be seen, modes with  $q > 2$  are characterized by two dominant branches which are shifted to higher magnetic field because of the increase of the cavity resonance frequency with  $q$ . This results in significant overlap of the modes on the lower magnetic field side of  $TE_{mp1}$  (ie., in the range 53-55 kG in the figure), and a spreading out of modes on the higher side. In addition, the modes on the higher magnetic field side have larger values of  $u^3/w^2$  and hence significantly reduced starting currents.

Figures 2 and 3 are examples of mode spectra associated with the operation of high frequency gyrotrons. Both figures were calculated using Eq. (9). The device parameters are: beam voltage = 65 kV, cavity length = 15 mm, frequency = 140 GHz,  $Q_T = 8 \pi (L/\lambda q)^2$  (see Eq. (12)), and  $w/u = 1.5$  at a magnetic field of 55.7 kG. The electron beam interacts with the second radial maximum of  $TE_{031}$  in Fig. 2, and with the only radial maximum of  $TE_{511}$  in Fig. 3. The only parameter that differs for the two figures is the cavity radius. The radius is adjusted so that the oscillation frequency is 140 GHz for the desired modes  $TE_{031}$  and  $TE_{511}$ .

Fig. 2 clearly demonstrates the severe mode competition that will be encountered when attempting to operate in higher order modes. Here one can see  $TE_{031}$ ,  $TE_{231}$ ,  $TE_{521}$ , and their associated higher  $q$  modes. Careful inspection reveals the

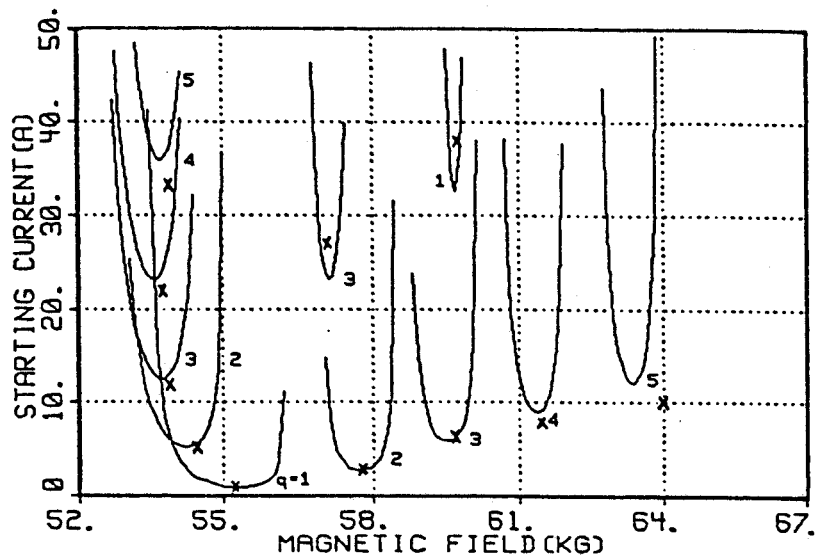


Fig. 1 Starting current plotted as a function of magnetic field for  $TE_{03q}$  modes with  $1 \leq q \leq 5$ . The x's indicate the minimum starting current points predicted by Eqs. (15), (17) and Table 1.

hierarchy of modes shown in Fig. 1. In order to achieve high efficiency in the  $TE_{031}$  mode, it will be necessary to operate on the lower magnetic field side of the gain curve, at approximately 54 kG. Fig. 2 suggests that stable, single mode operation might be difficult due to the strong overlap of the modes  $TE_{231}$  and  $TE_{032}$ . One possible solution is the use of damping that would selectively lower the  $Q_T$ 's of unwanted modes.

It has been suggested (5) that the use of whispering gallery modes, characterized by large  $m$  and  $p = 1$ , might alleviate the mode competition problem. This conclusion is supported by Fig. 3, which shows that the only modes severely overlapping with  $TE_{511}$  are its higher  $q$  modes. The primary reason for the absence of competing modes is that the RF fields of whispering gallery modes are localized near the cavity walls, and an electron beam interacting with this mode will not couple effectively with other modes whose RF field maxima are closer to the resonator axis.

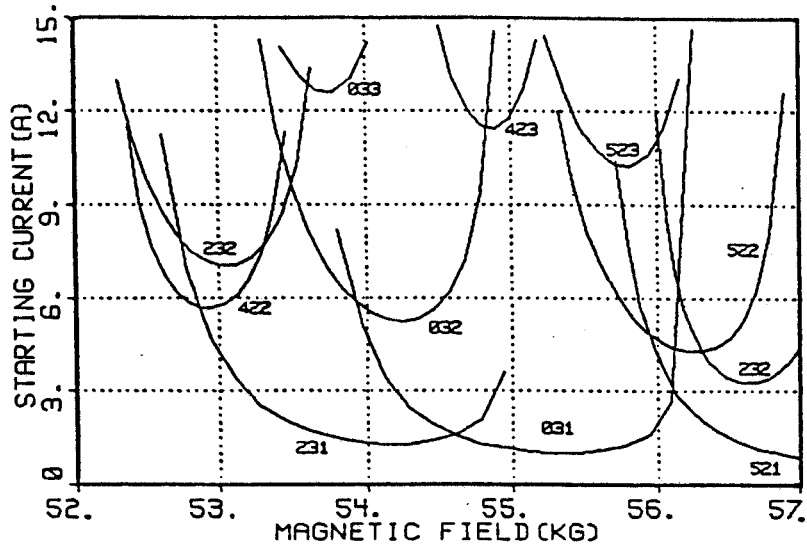


Fig. 2 Mode spectrum associated with 140 GHz operation in the  $TE_{031}$  mode. Cavity and beam parameters are given in the text. The electron beam interacts with the second radial maximum of the RF field.

### 3. Startup of a Gyrotion

In this section we will investigate the startup phase of a pulsed gyrotion (6). As a result of the time varying gun parameters, the magnetic field and starting current needed for self-excitation drastically change during this period. Therefore it is important that the gun parameters be carefully controlled in order that the desired mode is excited first. Due to the brevity of the startup period (typically lasting a few microseconds or less), only the cathode and control anode voltages can be altered appreciably in practice. The magnetic field cannot be changed on such a fast time scale. The beam current, which is set by the thermal emission limit of the gun, reaches its full value at gun voltages which are well below their final operating levels. Therefore, the magnetic field and beam current can be treated as fixed parameters during the startup phase.

Ideally, the startup scenario chosen should result in the excitation of the desired mode first, and should maintain

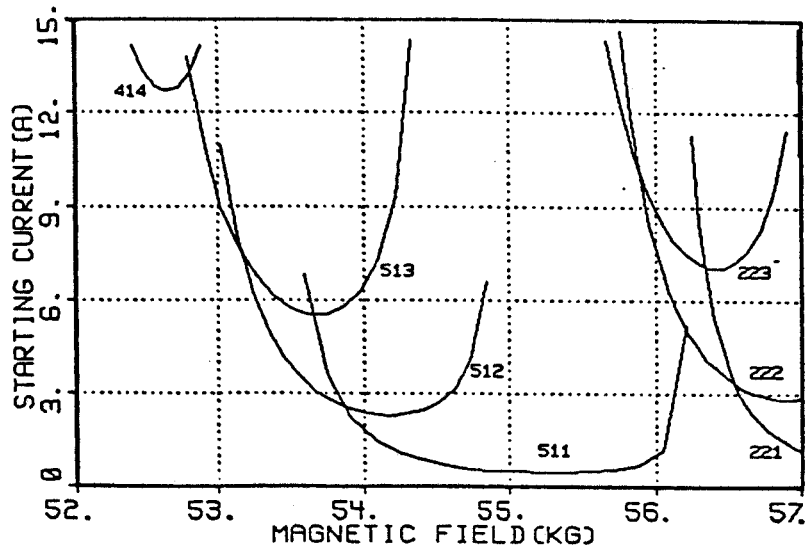


Fig. 3 Mode spectrum associated with the whispering gallery mode  $TE_{511}$ . Same device parameters as for Fig. 1, except the cavity radius has been decreased in order to keep the oscillation frequency at 140 GHz.

stable, single-mode operation thereafter. The analysis of mode stability requires a nonlinear treatment of the beam-field interaction and is beyond the scope of this paper. However, a number of studies have been done (7,8), and these indicate that once a mode is excited, it tends to suppress the initiation of subsequent modes. Therefore, the excitation of the desired mode first will help to ensure that stability is achieved. It is also desirable that the working mode be chosen in a region relatively free of competing modes. A good example of this is the whispering gallery mode discussed earlier in this paper.

We have analyzed various gyrotron startup scenarios by solving the linear theory (3) exactly on a computer. This allows us to generate mode charts quickly for a variety of gun voltages. Two methods of turn-on were investigated in detail. In one sequence, both the cathode and control anode voltages were varied to their final operating values in such a manner that their ratio remained constant. This can be accomplished in practice through the use of a resistance divider. This is shown for the case of the  $TE_{031}$  mode

discussed earlier in Figures 4a through 4d, where the final operating parameters are those associated with Figure 2. It should be noted that we have defined the cathode voltage  $U$  as the potential difference between ground and the cathode, and the anode voltage  $V_a$  as the difference between the control anode and the cathode. Thus we treat  $V_a$  and  $U$  as positive quantities, although in reality both voltages must be driven negative in order to generate an electron beam. Also, the value of  $V_a$  associated with Fig. 2 is 20 kV, which results in an electric field of  $5 \times 10^6$  V/m between the control anode and cathode.

In the second sequence, the cathode voltage  $U$  is held constant while  $V_a$  is ramped up from below cathode voltage to its final operating value. This might be accomplished through the use of two independently controlled voltage supplies, one CW and the other modulated. This scenario is shown in Figures 5a and 5b, where again TE<sub>031</sub> operation depicted in Fig. 2 has been chosen as the final operating point.

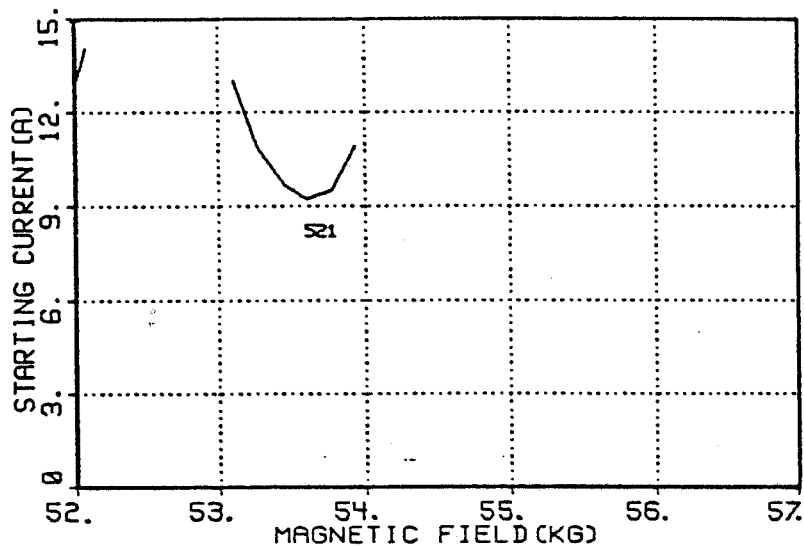


Fig. 4a)  $U = 35$  kV,  $V_a = 10.77$  kV



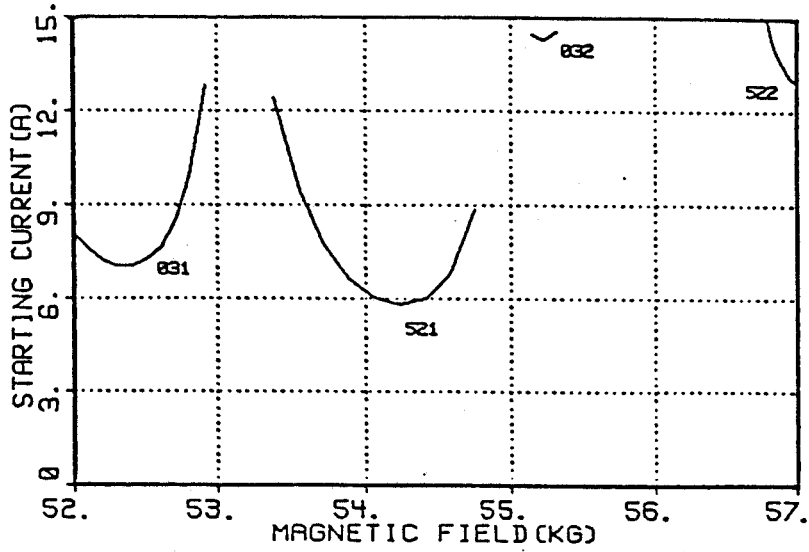


Fig. 4b)  $U = 40 \text{ kV}$ ,  $V_a = 12.31 \text{ kV}$

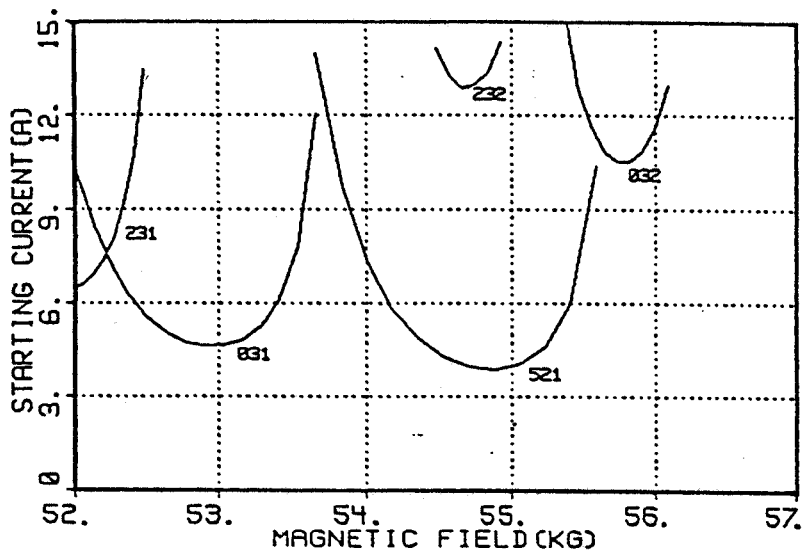


Fig. 4c)  $U = 45 \text{ kV}$ ,  $V_a = 13.85 \text{ kV}$

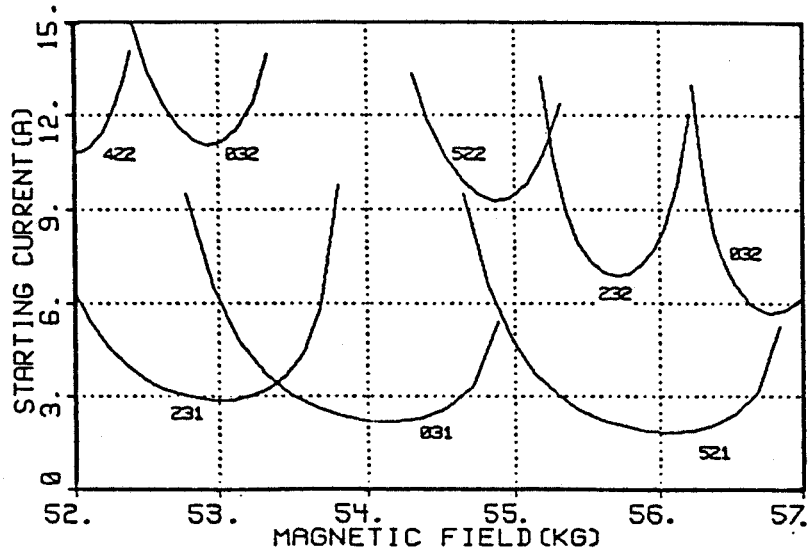


Fig. 4d)  $U = 55 \text{ kV}$ ,  $V_a = 16.92 \text{ kV}$

Figures 4 Sequence of graphs showing how the starting current and magnetic field associated with each mode vary as the cathode ( $U$ ) and anode ( $V_a$ ) voltages are changed. In this sequence,  $U$  and  $V_a$  are increased in such a manner that  $V_a/U$  remains constant. The device parameters and final gun voltages are those associated with Fig. 2.

Examining these two sets of graphs, one can see how dramatically the excitation regions shift during the startup phase. This is particularly true for the  $V_a/U = \text{constant}$  sequence. Here one can see the  $TE_{521}$  curve minimum shift from 53.5 kG to 57 kG as  $U$  increases from 35 to 65 kV. In addition the minimum starting current decreases from about 9.3 A to 1 A, primarily due to the fact that  $w/u$  increases as the gun voltages are raised to their final values.

In order to evaluate whether the desired mode will be excited first, the beam current and magnetic field must be chosen. We have selected 6 A in order to achieve 100 kW output power, and 54 kG based on efficiency calculations of Chu et.al. (9). Looking at the  $V_a/U = \text{constant}$  sequence of figures, one can observe that there is a real danger of exciting the  $TE_{521}$  mode first at  $U = 40 \text{ kV}$ , well before the

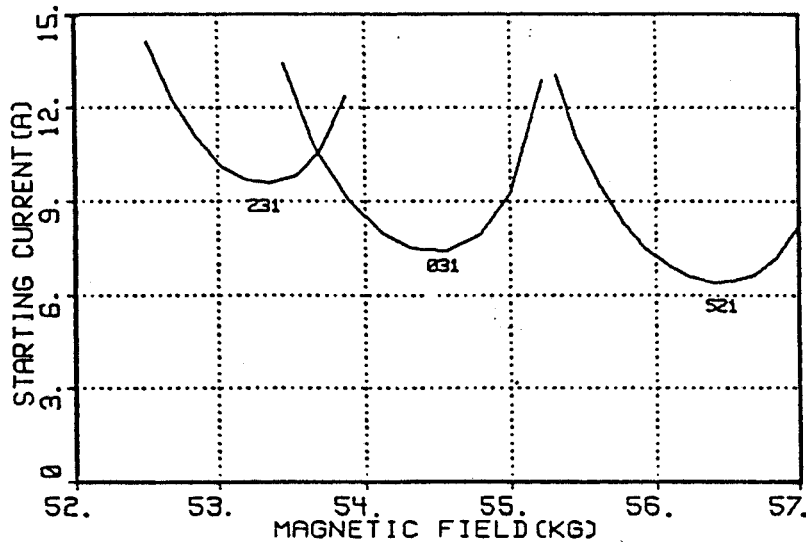


Fig. 5a)  $U = 65 \text{ kV}$ ,  $V_a = 15 \text{ kV}$

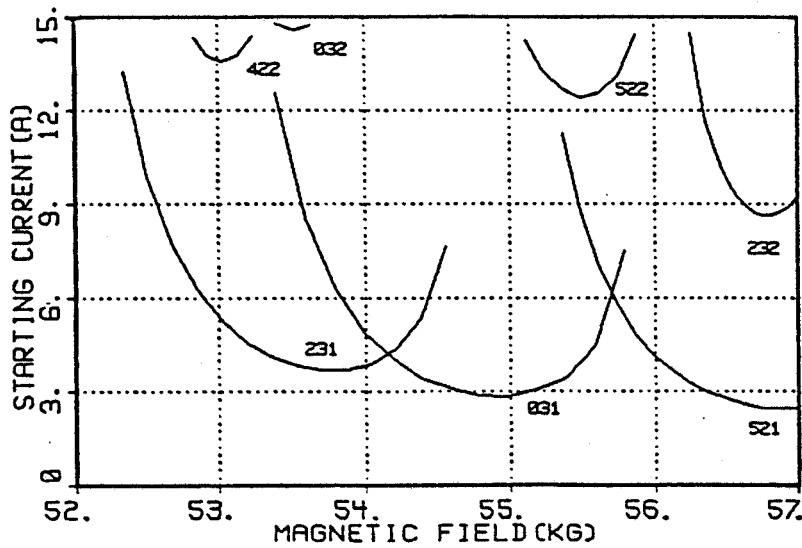


Fig. 5b)  $U = 65 \text{ kV}$ ,  $V_a = 17.5 \text{ kV}$

Figures 5 Similar sequence of graphs as in Fig. 4, except  $U$  is held fixed while  $V_a$  is varied. Again, the device parameters and final gun voltages are those given with Fig. 2.

$TE_{031}$  mode is excited at about  $U = 50$  kV. There are a number of possible ways of circumventing this problem. First, the diffractive  $Q$  for  $TE_{521}$  could be selectively lowered by modifying the resonator shape or output coupling, thus raising the starting current sufficiently to avoid oscillation. Here, one must avoid altering the  $Q_T$  of the  $TE_{031}$  mode as much as possible. A second approach would involve varying the radius of the electron beam in order to reduce coupling between the beam and RF field of the  $TE_{521}$  mode. As before, this would only be effective if strong beam coupling with the  $TE_{031}$  mode could be maintained. A final method is suggested by the second startup scenario. Rather than select a startup in which the excitation regions undergo large shifts in magnetic field, it would be desirable to choose a method in which the field associated with each drive remains relatively fixed, and only the minimum starting current is changing. As a result the neighboring parasitic modes would have less of an opportunity to be excited before the desired mode, as is illustrated in Figs. 5a and 5b. For this case, as  $V_a$  goes from 15 to 20 kV, the magnetic field associated with  $TE_{031}$  only shifts from 54.5 kG to 55.3 kG. The  $TE_{031}$  mode is excited just before the  $TE_{231}$  mode at  $V_a = 17$  kV. The primary reason for the smaller shifts associated with this startup is the fact that the parameter  $x_{MIN}$ , which determines the magnetic field required to excite a mode with the minimum beam current, is less sensitive to  $V_a$  than it is to  $U$ .

Once the beam current and magnetic field are fixed, it is possible to depict all possible startup methods on a single graph. This is shown in Fig. 6, where the regions of self-oscillation for a number of competing modes have been plotted as a function of  $U$  and  $V_a$ . The two scenarios,  $V_a/U = \text{constant}$  and  $U = \text{constant}$ , are indicated on the graph by lines I and II respectively. Notice how line I just intersects with the  $TE_{521}$  curve at  $U = 40$  kV, indicating that  $TE_{521}$  would be excited before the  $TE_{031}$  oscillation region is reached. In the case of startup II,  $TE_{031}$  is reached first, but the proximity of the  $TE_{231}$  curve might lead to mode competition difficulties. Fig. 6 indicates that the most favorable startup method would be represented by a curve that passes through the region between I and II. In practice, this would be accomplished by having the anode voltage rise lag somewhat behind the cathode voltage rise. If plotted in a manner similar to Figs. 5 and 6, this scenario would show the  $TE_{031}$  mode being excited on the higher magnetic field side of the excitation curve, away

from the TE<sub>231</sub> and TE<sub>521</sub> curves, and then the operating point would shift to the lower field side of the TE<sub>031</sub> curve in order that high efficiency operation might be achieved.

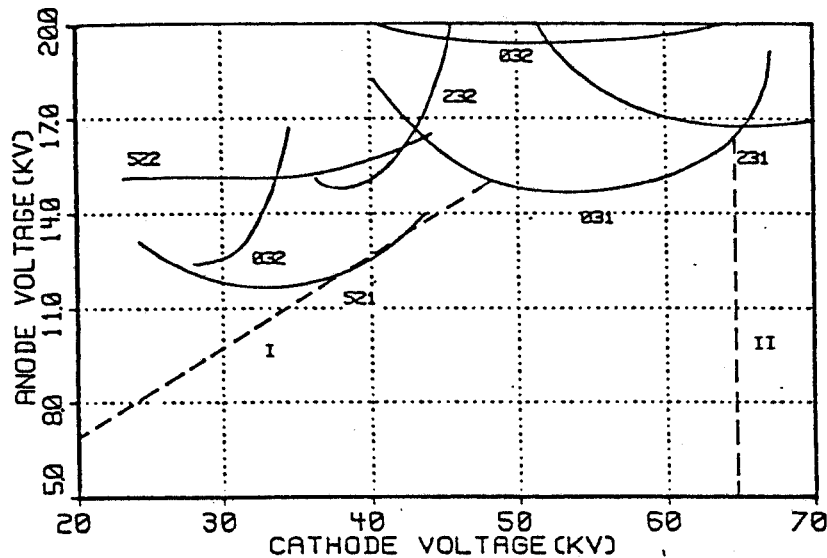


**Figure 6** Regions of self-oscillation plotted as a function of the cathode and anode voltage. Curves based on a beam current of 6 A and a resonator magnetic field of 54 kG. Line I represents the startup of Fig. 4 ( $V_a/U = \text{constant}$ ), while line II is associated with the startup of Fig. 5 ( $U$  fixed,  $V_a$  increasing).

#### 4. Conclusions

In this paper, we have derived a simple theory of mode excitation which, in contrast to the Doppler approximation often used, is in reasonably good agreement with numerical calculations based on the exact linear theory. For a TE<sub>mpq</sub> mode, there can in theory be an infinite number of excitation branches corresponding to a higher order series of bunching and unbunching processes. In general, there are only  $q$  strong branches of excitation for a TE<sub>mpq</sub> mode. For  $q > 2$ , two of these branches predominate and correspond roughly to the interaction between the electron beam and the forward and backward RF waves in the resonator.

For  $q = 1$ , only the backward wave interaction is strong.

If  $Q$  is held constant, the minimum starting current of a  $TE_{mpq}$  mode is found to be roughly independent of  $q$  for the main excitation branches. However, for cavities designed for operation in a  $q = 1$  mode, the diffractive  $Q$  decreases roughly as  $q^2$ , which accounts for the high starting currents generally assigned to high  $q$  modes. The magnetic field at which the minimum starting current occurs does vary with  $q$ , and this dependence must be taken into account when constructing a mode spectrum. Using the exact linear theory (3), it is found that the construction of such a spectrum is most easily accomplished by relating the current and magnetic field required for self-oscillation of the  $q \neq 1$ ,  $TE_{mpq}$  mode to the corresponding parameters for the nearby  $TE_{mpl}$  mode. Table I contains all the necessary information to do this. A complete mode chart can then be obtained by relating the  $q = 1$  modes to one another. One representative spectrum, the band of modes around  $TE_{031}$  as seen in Fig. 2, indicates how severe mode competition will be for high frequency operation. One possible solution is the selection of a whispering gallery mode as the working mode (5). In this case, coupling between the electron beam and spurious modes tends to be reduced due to the location of the beam near the cavity wall.

In our analysis of the startup phase of a pulsed gyrotron, it was found that holding the cathode voltage fixed while raising the control anode voltage was a better method of turn-on than raising both voltages in such a manner that their ratio remained constant. In the latter approach, the beam current and magnetic field associated with each mode excitation curve undergo large changes as the gun voltages are varied. As a result, it is difficult to choose a set of final operating parameters that does not result in spurious mode excitation during startup. However, if the cathode voltage is held fixed during turn-on the shifts in magnetic field of the excitation curves are appreciably reduced, and this gives neighboring modes less opportunity to be accidentally triggered. The primary reason for the smaller magnetic field shifts associated with this startup is the fact that the parameter  $x$ , which determines the field needed to excite a mode (see Eq. (5)), is much less sensitive to the anode than to the cathode voltage.

In the present discussion of the effect of voltage variation on mode excitation, it was assumed that the

electron beam parameters varied smoothly with voltage in a manner defined by adiabatic theory. In practice, this smooth variation may not be achieved. This would result in a somewhat different sequence of mode excitation. The present results should therefore be considered as illustrative examples rather than exact, quantitative results. Also, the analytic theory presented in this paper was derived for a cavity with a sinusoidal variation of the RF field in the axial direction of the resonator. Many of the experiments which are being conducted at present utilize tapered cavities in order to achieve enhanced efficiency and increased mode separation. For tapered cavities, the mode excitation results presented in this report could be significantly altered. However, many of the qualitative features of the present analysis should still apply.

#### References

1. V. A. Flyagin, A. V. Gaponov, M. I. Petelin and V. K. Yulpatov, IEEE Trans. Microwave Theory and Tech. MTT-25 (1977) 514.
2. J. L. Hirshfield and V. L. Granatstein, IEEE Trans. Microwave Theory and Tech. MTT-25 (1977) 522.
3. K. E. Kreischer and R. J. Temkin, Int. J. Infrared and Millimeter Waves 1 (1980) 195.
4. S. N. Vlasov, G. M. Zhislin, I. M. Orlova, M. I. Petelin and G. G. Rogacheva, Radiophysics and Quantum Electron. 12, No. 8 (1969) 972.
5. Yu. V. Bykov, A. F. Gol'denberg, L. V. Nikolaev, M. M. Ofitserov, and M. I. Petelin, Radiophysics and Quantum Electronics 18, No. 1 (1975) 141.
6. G. S. Nusinovich, Elektronnaya Tekhnika, Ser 1, Elektronika SVCh, No. 3 (1974) 44.
7. I. G. Zarnitsyna, G. S. Nusinovich, Radiophysics and Quantum Electronics 17, No. 12 (1974) 1418.
8. G. S. Nusinovich, Radiophysics and Quantum Electronics 19, No. 12 (1976) 1301.
9. K. R. Chu, M. E. Read, and A. K. Ganguly, IEEE Trans. Microwave Theory and Tech. MTT-28 (1980) 318.